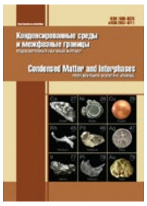

ISSN 1606-867X (Print)
ISSN 2687-0711 (Online)
Condensed Matter and Interphases
Kondensirovannye Sredy i Mezhfaznye Granitsy
https://journals.vsu.ru/kcmf/

Original articles

Research article
https://doi.org/10.17308/kcmf.2025.27/13019

Study of photoluminescence kinetics in bulk GaPN and GaPNAs layers on silicon substrates grown by molecular beam epitaxy

E. V. Nikitina[1,2], A. K. Kaveev[1], V. V. Fedorov[2], E. V. Pirogov[2], A. M. Nadtochiy[3], E. I. Vasilkova[2]✉, N. V. Kryzhanovskaya[3], M. S. Sobolev[2]

[1]Ioffe Institute,
26 Polytechnicheskaya st., St. Petersburg 194021, Russian Federation

[2]Alferov University,
8/3 Khlopina st., St. Petersburg 194021, Russian Federation

[3]HSE University Saint Petersburg,
16 Soyuz Pechatnikov st., St. Petersburg 194100, Russian Federation

Abstract

Objective: The aim of this work is to study bulk GaPN and GaPNAs layers grown by molecular beam epitaxy on silicon substrates. The optical properties of the heterostructures were investigated using photoluminescence. The technique of time-resolved photoluminescence (or photoluminescence kinetics) was employed to evaluate the carrier lifetime in bulk GaPN and GaPNAs layers.

Experimental: An investigation of the influence of the buffer layer on the heterostructure characteristics was conducted. The photoluminescence intensity in the bulk GaPN layer was found to be virtually identical for heterostructures employing either a buffer layer grown by Migration-Enhanced Epitaxy (MEE-GaP buffer) or a GaP buffer layer grown with a gradual temperature ramp from 450 to 600 °C.

Conclusion: It was shown that the lifetime of minority carriers in the bulk GaPN layer grown on a silicon substrate is determined to a greater extent by defects introduced during the nitrogen incorporation into the GaP lattice, rather than by defects caused by growth on silicon substrate.

Keywords: Dilute nitrides, GaPN(As), Photoluminescence, Silicon substrate

Funding: The study was supported by the Russian Science Foundation No. 23-79-00032 (https://rscf.ru/project/23-79-00032/). The optical investigation of time-resolved photoluminescence was conducted on a unique setup "Complex optoelectronic unit of the National Research University Higher School of Economics - St. Petersburg".

For citation: Nikitina E. V., Kaveev A. K., Fedorov V. V., Pirogov E. V., Nadtochiy A. M., Vasilkova E. I., Kryzhanovskaya N. V., Sobolev M. S. Study of photoluminescence kinetics in bulk GaPN and GaPNAs layers on silicon substrates grown by molecular beam epitaxy. *Condensed Matter and Interphases*. 2025;27(3): 433–440. https://doi.org/10.17308/kcmf.2025.27/13019

Для цитирования: Никитина Е. В., Кавеев А. К., Федоров В. В., Пирогов Е. В., Надточий А. М., Василькова Е. И., Крыжановская Н. В., Соболев М. С. Исследование кинетики фотолюминесценции объемных слоев GaPN и GaPNAs на подложках кремния, выращенных методом молекулярно-пучковой эпитаксии. Конденсированные среды и межфазные границы. 2025;27(3): 433–440. https://doi.org/10.17308/kcmf.2025.27/13019

✉ Elena I. Vasilkova, e-mail: elenvasilkov@gmail.com

1. Introduction

Solid solutions of ternary and quaternary $A^{III}B^{V}N$ compounds with a nitrogen mole fraction of a few percent form a new class of promising materials for optoelectronic devices, known as "dilute nitrides". These solid solutions are promising for fabricating silicon-based optoelectronic devices, such as LEDs, photodetectors, lasers, and high-efficiency multijunction solar cells [1]. The addition of less than one percent of nitrogen to gallium phosphide (GaP) lattice results in the formation of direct-bandgap GaPN material. Increasing the nitrogen mole fraction in ternary and quaternary $A^{III}B^{V}N$ compounds leads to a significant reduction in the bandgap energy accompanied by a decrease in the lattice constant [2, 3]. This unusual property of dilute nitrides arises from the substitution of a small fraction of group V elements (P and/or As) with nitrogen atoms, which substantially modifies the conduction band, splitting it into two non-parabolic subbands (E– and E+). The Band Anticrossing Model (BACm), describing the formation of this new band structure, was proposed and developed in [4]. Adding arsenic atoms to GaPN to create a quaternary solid solution allows tuning the bandgap energy over a wide range (1.5–2.0 eV) while maintaining lattice matching with silicon substrates through variation of group V elements ratios in GaPNAs [5]. However, experimental studies reveal low minority carrier lifetimes in GaPNAs active layers grown on gallium phosphide and silicon substrates by MOCVD [6] and MBE [7], attributed to the high density of defects. Reducing the defect densities in GaPN(As) solid solutions grown on silicon substrates can be achieved through the optimization of the buffer layer design and epitaxial growth parameters for the dilute nitride layers. The challenge in forming gallium phosphide buffer layers on the silicon surface stems from potential chemical reactions at the interface, where gallium atoms can etch the silicon surface, leading to pit formation [8]. Currently, a commonly used approach to creating a transition layer between the silicon substrate and the active layer based on dilute nitrides is the Migration-Enhanced Epitaxy (MEE) GaP buffer [9]. The MEE technique involves alternating the phosphorus and gallium flux supply to the substrate at lower growth temperatures. However, the implementation of this technique inevitably reduces the service life of the shutters in a molecular beam epitaxy system [10]. An alternative approach for epitaxial growth of GaP buffer layers on silicon substrate, as demonstrated in [11], involves growing a buffer layer composed of low-temperature (440 °C) and high-temperature (580 °C) bulk GaP sublayers.

In this work, we studied the characteristics of heterostructures with active layers based on bulk ternary GaPN or quaternary GaPN(As) solid solutions, grown by molecular beam epitaxy (MBE) on silicon substrates. The characterization methods employed photoluminescence, X-Ray diffractometry, as well as time-resolved photoluminescence (photoluminescence kinetics).

2. Experimental

The studied epitaxial structures were obtained using the MBE method using a Veeco Gen III setup with a radio frequency (RF) inductively coupled nitrogen plasma source on Si (001) substrates with a 4° off-cut toward the [100] direction. The use of [100]-misoriented silicon substrates was necessary to prevent the appearance of antiphase domains at the silicon–gallium phosphide heterointerface. For the same purpose, a phosphorus monolayer was deposited on the silicon surface after substrate annealing in the growth chamber.

The samples studied consisted of a bulk layer of ternary or quaternary GaPN(As) solid solution grown on a buffer layer. Sample #1 featured a MEE-GaP buffer layer based on 45 periods of alternating sublayers of gallium and phosphorus [9], followed by 50 nm GaP layer grown at 450 °C. The buffer layer of other samples (#2, #3, #4) incorporated a thin (1 nm) AlP sublayer deposited at 450 °C, followed by GaP layer grown with a gradual temperature ramp to 600 °C. The AlP sublayer in these samples prevents etching of the silicon surface by gallium atoms. The GaPN bulk layers for samples #1 and #2 were formed under identical growth conditions with a nitrogen flow rate of 0.3 ml/min. For Sample #3, the power of the RF nitrogen plasma source was increased from 225 W (used for #1 and #2) to 250 W with a nitrogen flow of 0.35 ml/min to achieve higher nitrogen mole fraction in GaPN layer. Sample #4 contained GaPNAs layer, grown with the same nitrogen flow and RF nitrogen plasma source power of 250 W and an arsenic flux to total group V flux ratio (As+P) of 0.1.

Diffraction rocking curves were obtained using a DRON-8 X-Ray diffractometer equipped with a BSV 29 fine-focus X-ray tube. The anode material was copper, utilizing $K\alpha 1$ radiation (λ = 1.5405 Å). Photoluminescence spectra were measured using an Accent Optical Technologies setup. The structures were studied by photoluminescence (PL) spectroscopy in the spectral range of 500–800 nm at room temperature. Optical excitation was provided by a continuous-wave solid-state laser operating at 266 nm, with an excitation power density of 12 W/cm^2.

The study of the time resolved photoluminescence was carried out by the up-conversion method using a FOG-100-DX-IR device for differential fluorescence kinetics measurements in the visible range. Laser pulses with a duration of 120 fs, a frequency of 80 MHz, and a wavelength of 780 nm, generated by a tunable titanium-sapphire laser CoherentMira 900D with a maximum average power of 1.5 W were used for gating and exciting the samples. To implement the optical excitation of the samples, the excitation pulse was passed through a frequency-doubling system based on a nonlinear BBO (β-BaB_2O_4) crystal. Thus, the sample excitation during time-resolved photoluminescence investigation was performed at a wavelength of 395 nm, while signal gating was produced by the primary pulse with a wavelength of 780 nm.

3. Results and discussion

Fig. 1 presents the room temperature photoluminescence spectra of the studied samples. Samples #1 and #2 featured different buffer layers, but the GaPN layer growth parameters were identical. The PL data revealed that the PL intensity of Sample #2 was 20 % higher, while its PL peak was redshifted. This suggests that Sample #2 achieved improved nitrogen incorporation into the GaP lattice, and the gradient buffer layer contributed to the formation of GaPN layers with enhanced photoluminescence relative to the conventional MEE-GaP buffer layer. As will be shown further by X-ray diffraction analysis, this difference was attributed to distinct strain relaxation mechanisms.

The nitrogen flux during the growth of sample #3 was increased compared to samples #1 and #2. The photoluminescence peak energy of the samples decreased with rising nitrogen

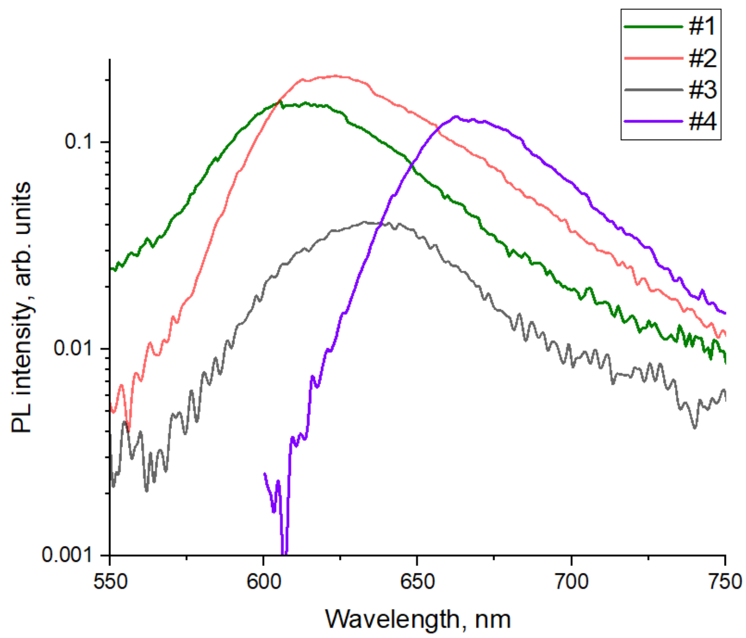

Fig. 1. Room-temperature photoluminescence spectra of bulk ternary GaPN (Samples #1, #2, #3) and quaternary GaPNAs (Sample #4) solid solutions

concentration in the epitaxial layer, corresponding to bandgap reduction (emission wavelength redshift). With an increase in nitrogen content in a solid solution there was typically a drastic fall in the photoluminescence peak intensity, as shown in [12]. This may be attributed to the formation of deep levels due to nitrogen incorporation, which act as nonradiative recombination centers. In our case, the peak PL intensity of Sample #3 was over 5 times lower relative to Sample #2. Additionally, PL intensity reduction in Sample #3 can be attributed to the fact that the bulk GaPN layer was no longer lattice-matched to silicon, as confirmed by X-Ray diffraction and will be discussed further, see Fig. 2.

Incorporating arsenic atoms into the GaPN solid solution enables lattice matching to silicon through tuning of group V element ratios, since nitrogen reduces the lattice constant, while arsenic increases it. In Sample #4, grown with the nitrogen source parameters similar to that of Sample #3 and an As to P flux ratio of 0.1, arsenic incorporation resulted in a threefold increase in PL intensity of Sample #4 compared to Sample #3, accompanied by a PL peak wavelength shift towards 665 nm.

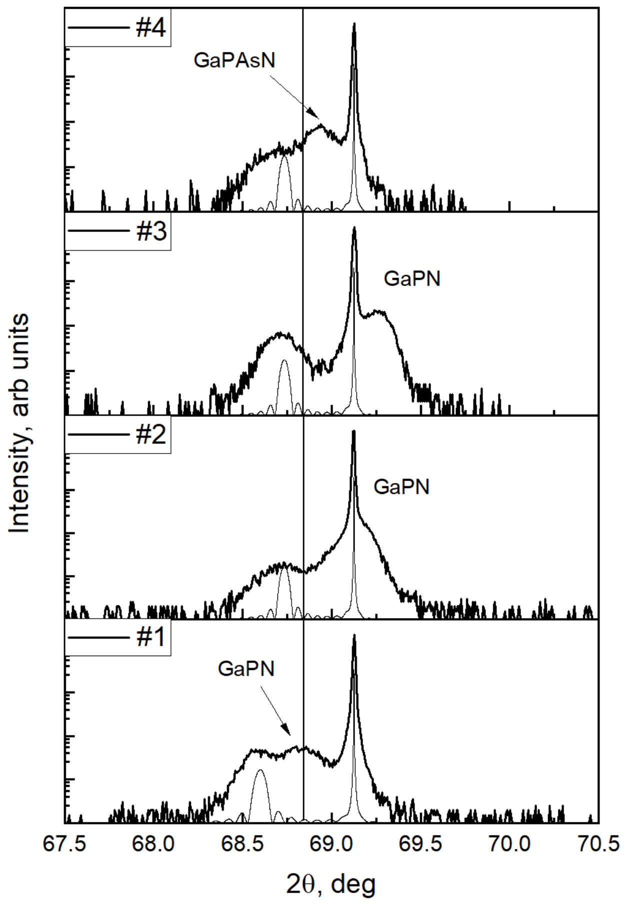

Fig. 2. X-Ray diffraction rocking curves around the symmetrical Si reflection for bulk ternary GaPN (Samples #1, #2, #3) and quaternary GaPNAs (Sample #4) solid solutions

Fig. 2 shows the X-Ray rocking curves of the examined samples measured near the symmetrical Si reflection. The black vertical line indicates the theoretical position of the fully relaxed GaP diffraction peak. The calculated X-Ray rocking curves for GaP layers with different degrees of strain relaxation on silicon substrates are also presented.

The calculated position of the GaP diffraction peak in Sample #1 corresponded to a fully strained layer, while an analysis of the GaPN peak position reveals a nitrogen content of 1.5 %. The GaP diffraction peaks in Samples #2, #3 and #4 let us evaluate an approximate strain relaxation degree of ~ 55 %, as determined by comparing experimental data with the theoretical simulation. This can be attributed to dislocation formation during the initial stages of growth, which induced partial strain relaxation in the epitaxial layers of these samples. Consequently, the lattice parameter of GaP epitaxial layer approaches that of a fully relaxed GaP layer. Despite the significant difference in diffraction peak positions, the nitrogen mole fraction in the GaPN layer of Sample #1 approached that of Sample #2, where the nitrogen content reached approximately 1.8 %. This difference arose from the rightward shift of diffraction peaks due to strain relaxation in epitaxial layers, which is most prominent in Sample #3. The calculated nitrogen mole fraction in the GaPN layer of this sample was approximately 2.24 %, however, the GaPN diffraction peak maximum was significantly shifted towards higher angles, whereas the nitrogen content of approximately 2.1 % should have resulted in a peak alignment between the GaPN layer and silicon substrate. In Sample #4, a phenomenon of lattice parameter expansion was observed upon incorporation of 10 % arsenic into the GaPN(As) layer, while maintaining the same nitrogen mole fraction as in Structure #3.

Table 1 presents the values of the nitrogen molar fraction, as determined from X-Ray diffraction rocking curves analysis and the Band Anticrossing Model calculations.

A previous study [13] demonstrated that the efficiency of multijunction solar cells based on GaPNAs solid solutions as top junctions and silicon substrates as bottom junctions is also heavily influenced by such a parameter of the material as the minority carrier lifetime. Therefore, we performed studies of the photoluminescence kinetics of heterostructures with bulk GaPN layers at both room temperature (300 K) and cryogenic temperature (5 K).

Figure 3 shows the room-temperature PL intensity decay measured for the light wavelength corresponding to the PL intensity peak.

All samples studied exhibited a PL with a relatively short decay time, though the decays do not show a monoexponential behavior. The PL decline times, evaluated as the 1/e maximum intensity level, estimated approximately 40 ps for the samples containing GaPN layer and 11 ps for the sample with a GaPNAs layer. Bulk GaPN layers, grown on gallium phosphide substrates, demonstrated a comparable minority carrier lifetime of 70–100 ps [14]. Therefore, short minority carrier lifetimes in GaPN layers grown on silicon is determined primarily by defects introduced during the nitrogen incorporation into the GaP lattice, rather than by defects associated with growth on silicon substrate.

Time-resolved photoluminescence studies were performed at a temperature of 5 K. The PL

Table 1. Key characteristics of GaPN(As) heterostructures grown on silicon substrates

Sample	PL wavelength, nm	GaPNAs solid solution composition			$\tau_{1/e}$, ps	
		N molar fraction		As molar fractionAs	5 K	300 K
		PL	XRD			
1	612	0.0145	0.0149	–	2867	42
2	620	0.0175	0.018	–	3678	44
3	636	0.022	0.0224	–	488	35
4	663	0.022	0.0224	0.1	–	11

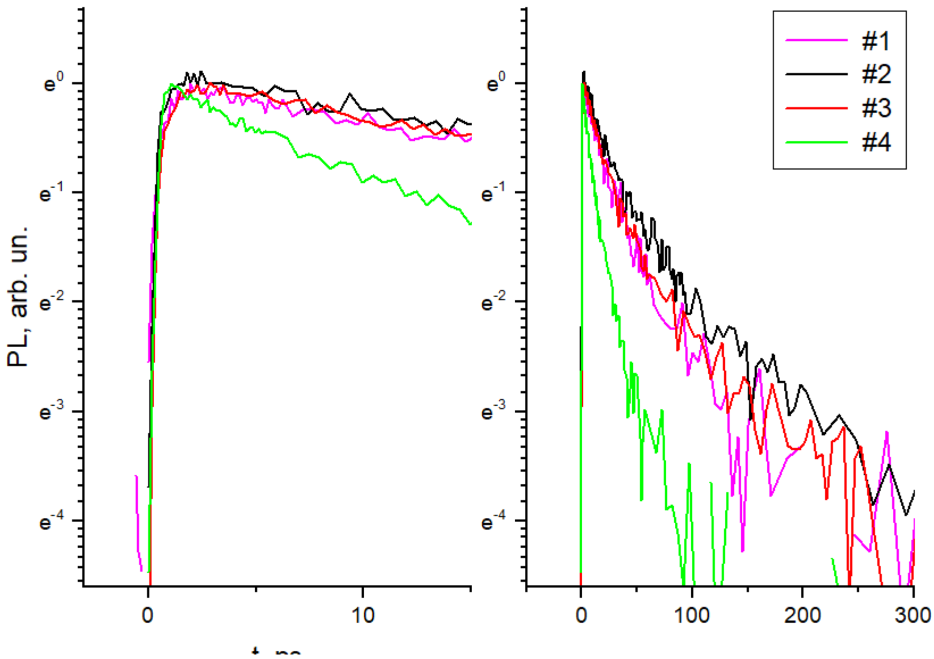

Fig. 3. Normalized time-resolved PL intensity decays for GaPN-based active regions, obtained at 300 K for the excitation wavelength of 620 (Samples #1, #2, #3) and 650 nm (Samples #4), displayed in two time windows (left panel – 0-15 ps, right panel – 0-300 ps)

decay kinetics for the samples with a bulk GaPN layer (Samples #1, #2 and #3) are shown in Fig. 4. The left panel shows the initial part of the PL decay, while the right panel presents the complete investigated time range. It should be noted that all decay curves exhibit a persistent background signal - detectable PL intensity preceding the arrival of each excitation pulse. This indicates the presence of slow mechanisms of PL decline with characteristic times exceeding the interval between the excitation pulses.

A comparative analysis of PL decay kinetics at room temperature (Fig. 3) and cryogenic temperature 5 K (Fig. 4) reveals a pronounced increase in PL decline time for all samples at lower temperatures. For instance, Sample #3 exhibits a 1/e decay time value increase to 488 ps when measurement conditions were changed from room temperature to 5 K. Moreover, the low temperature PL decays follow monoexponential kinetics. Thus, one can conclude that temperature decrease drastically extends minority carrier lifetimes in GaPN structures grown on silicon substrates.

Table 1 presents the key properties of the studied heterostructures containing bulk GaPN(As) layers grown on silicon substrates.

4. Conclusion

In this study, we investigated heterostructures containing bulk layers based on ternary GaPN and quaternary GaPNAs solid solutions grown by MBE on silicon substrates. Two buffer layer configurations were considered: a MEE-GaP buffer and a low-temperature GaP buffer with a gradient temperature ramp. It was shown the low-temperature gradient buffer layer exhibited partial elastic strain relaxation with a relaxation degree of about 55%. This strain relaxation led to an increase in the mole fraction of nitrogen incorporated in the GaP matrix, resulting in a redshift of the photoluminescence peak. An increase in the nitrogen flux led to a higher nitrogen mole fraction in the GaPN solid solution, a shift of the photoluminescence peak position to longer wavelengths, and a sharp drop of PL intensity. The addition of arsenic to a GaPN solid solution to create a quaternary solid solution,

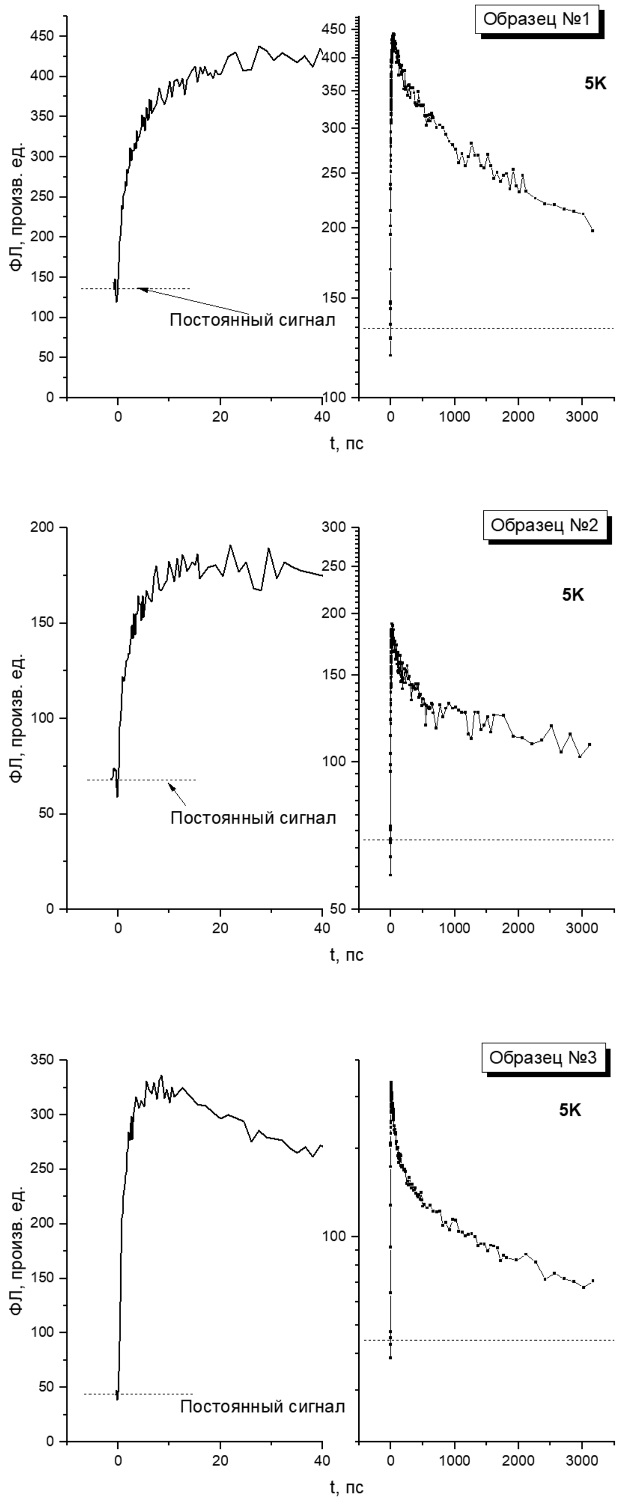

Fig. 4. Time-resolved PL intensity decays for GaPN-based active regions, obtained at 5 K for the excitation wavelength of 620 nm, displayed in two time windows (left panel – 0–40 ps, right panel – 0–3000 ps)

$GaP_{0.88}N_{0.02}As_{0.1}$, allowed a PL maximum at a wavelength of 663 nm at room temperature to be achieved, while the PL intensity increases threefold compared to $GaP_{0.98}N_{0.02}$.

This study investigated the dependence of photoluminescence kinetics in studied heterostructures on the composition of bulk GaPN and GaPNAs layers. At room temperature, the PL intensity decay time, determined at the 1/e maximum intensity level, measured approximately 40 ps for samples with GaPN layers and 11 ps for a sample with a GaPNAs layer. Reducing the PL kinetics measurement temperature drastically increased minority carrier lifetimes in GaPN structures grown on silicon substrates.

Contribution of the authors

The authors contributed equally to this article.

Conflict of interests

The authors declare that they have no known competing financial interests or personal relationships that could have influenced the work reported in this paper.

References

1. Henini M. *Dilute nitride semiconductors*. Elsevier; 2005. https://doi.org/10.1016/B978-0-08-044502-1.X5000-8

2. Shan W., Walukiewicz W., Yu K. M., ...Tu C. W. Nature of the fundamental band gap in GaNxP1−x alloys. *Applied Physics Letters*. 2000;76: 3251. https://doi.org/10.1063/1.126597

3. Buyanova I. A., Pozina G., Bergman J. P., Chen W. M., Xin H. P., Tu C. W. Time-resolved studies of photoluminescence in GaN_xP_{1-x} alloys: evidence for indirect-direct band gap crossover. *Applied Physics Letters*. 2002;81(1): 52–54. https://doi.org/10.1063/1.1491286

4. Kent P. R. C., Zunger A. Theory of electronic structure evolution in GaAsN and GaPN alloys. *Physical Review B*. 2001;64(11): 115208. https://doi.org/10.1103/PhysRevB.64.115208

5. Geisz J. F., Friedman D. J. III–N–V semiconductors for solar photovoltaic applications. *Semiconductor Science and Technology*. 2002;17(8): 769–777. https://doi.org/10.1088/0268-1242/17/8/305

6. Geisz J. F., Olson J. M., Friedman D. J., Jones K. M., Reedy R. C., Romero M. J. Lattice-matched GaNPAs-on-silicon tandem solar cells. In: *Conference Record of the Thirty-first IEEE Photovoltaic Specialists Conference. 2005*. (pp. 695–698). IEEE. https://doi.org/10.1109/PVSC.2005.1488226

7. Baranov A. I., Gudovskikh A. S., Nikitina E. V., Egorov A. Y. Photoelectric properties of solar cells based on GaPNAs/GaP heterostructures. *Technical Physics Letters*. 2013;39: 1117–1120. https://doi.org/10.1134/S1063785013120171

8. Khoury M., Tottereau O., Feuillet G., Vennégués P., Zúñiga-Pérez J. Evolution and prevention of meltback etching: Case study of semipolar GaN growth on patterned silicon substrates. *Journal of Applied Physics*. 2017;122(10): 105108. https://doi.org/10.1063/1.5001914

9. Takagi Y., Yonezu H., Samonji K., Tsuji T., Ohshima N. Generation and suppression process of crystalline defects in GaP layers grown on misoriented Si(100) substrates. *Journal of Crystal Growth*. 1998;187(1): 42–50. https://doi.org/10.1016/S0022-0248(97)00862-2

10. Volz K., Beyer A., Witte W., Ohlmann J., Németh I., Kunert B., Stolz W. GaP-nucleation on exact Si (001) substrates for III/V device integration. *Journal of Crystal Growth*. 2011;315(1): 37–47. https://doi.org/10.1016/j.jcrysgro.2010.10.036

11. Fedorov V. V., Fedina S. V., Kaveev A. K., Kirilenko D. A., Faleev N. N., Mukhin I. S. The formation of single-domain gallium phosphide buffer layers on a silicon substrate without the use of migration enhanced epitaxy trchnique. *St. Petersburg Polytechnical University Journal: Physics and Mathematics*. 2024;17(2): 120–133. https://doi.org/10.18721/JPM.17209

12. Rumyantsev O. I., Brunkov P. N., Pirogov E. V., Egorov A. Yu. Study of defects in heterostructures with GaPAsN and GaPN quantum wells in the GaP matrix. *Semiconductors*. 2010;44(7): 893–897. https://doi.org/10.1134/s1063782610070110

13. Kudryashov D. A., Gudovskikh A. S., Nikitina E. V., Egorov A. Yu. Design of multijunction GaPNAs/Si heterostructure solar cells by computer simulation. *Semiconductors*. 2014;48(3): 381–386. https://doi.org/10.1134/s1063782614030154

14. Nikitina E. V., Sobolev M. S., Pirogov E. V., ... Kryzhanovskaya N. V. Photoluminescence of GaPNAs/GaP(N) superlattices and bulk GaPN layers on GaP substrates. *Condensed Matter and Interphases*. 2024;26(3): 490–495. https://doi.org/10.17308/kcmf.2024.26/12224

Information about the authors

Ekaterina V. Nikitina, Cand. Sci. (Phys.–Math.), Lead Researcher, Alferov University (Saint Petersburg, Russian Federation).

https://orcid.org/ 0000-0002-6800-9218
mail.nikitina@mail.ru

Andrey K. Kaveev, Dr. Sci. (Phys.–Math.), Leading Researcher, Ioffe Institute (Saint-Petersburg, Russian Federation).

https://orcid.org/0000-0002-3640-677X
kaveev@mail.ioffe.ru

Maxim S. Sobolev, Cand. Sci. (Phys.–Math.), Head of the Laboratory, Alferov University (Saint Petersburg, Russian Federation).

https://orcid.org/0000-0001-8629-2064
sobolevsms@gmail.com

Evgeny V. Pirogov, Researcher, Alferov University (Saint Petersburg, Russian Federation).

https://orcid.org/0000-0001-7186-3768
zzzavr@gmail.com

Alexey M. Nadtochiy, Cand. Sci. (Phys.–Math.), Leading Researcher, HSE University (Saint Petersburg, Russian Federation).

https://orcid.org/0000-0003-0982-907X

anadtochiy@hse.ru

Elena I. Vasilkova, postgraduate student, Engineer, Alferov University (Saint Petersburg, Russian Federation).

https://orcid.org/0000-0002-0349-7134

elenvasilkov@gmail.com

Natalia V. Kryzhanovskaya, Dr. Sci. (Phys.–Math.), Head of the laboratory, HSE University (Saint Petersburg, Russian Federation).

https://orcid.org/0000-0002-4945-9803

nkryzhanovskaya@hse.ru

Received October 28, 2024; accepted after reviewing November 11, 2024; accepted for publication November 15, 2024; published online September 25, 2025.